encit 2020

ABCM
Associação Brasileira de Engenharia e Ciências Mecânicas

18th Brazilian Congress of Thermal Sciences and Engineering
November 16–20, 2020 (Online)

ENC-2020-0375
SENSITIVITY OF THE BRAYTON CYCLE EFFICIENCY AND EMISSION PARAMETERS TO THE RECUPERATOR EFFECTIVENESS THROUGH A NUMERICAL MODEL BASED ON EQUILIBRIUM CONSTANTS

André Henrique Ávila de Souza
Universidade Federal da Grande Dourados, Dourados - MS
andrehenriqueavila@gmail.com

Ricardo A. V. Ramos
IPBEN-FEIS/UNESP, Ilha Solteira - SP
ricardo.ramos@unesp.br

Augusto Salomão Bornschlegell
Universidade Federal da Grande Dourados, Dourados - MS
augustosalomao@ufgd.edu.br

Abstract. *In a simple Brayton cycle, the combustion gases leave the turbine towards the atmosphere at high temperature, wasting energy that could be used. Thus, it is usual to implement mechanisms to take advantage of part of the energy that would be lost, improving the thermal efficiency of the cycle. The present work proposes a numerical model of a thermoelectric plant operating the Brayton cycle with recuperator and also considering combustion. The combustion products are modelled through chemical equilibrium. Computational modelling is implemented through Scilab © routines using real input data. Based on the results, a comparative study is carried out between the simple Brayton cycle and the recuperated Brayton cycle. Then, the sensitivity of the cycle thermal efficiency by varying the recuperator's effectiveness is discussed, as well as the variation in the emission of pollutant gases.*

Keywords: *Brayton cycle, recuperator, combustion, thermodynamics*

1. INTRODUCTION

The Brayton cycle was developed by George Brayton, in the 19th century, for piston engines (Çengel and Boles, 2007). Currently, the most common use are gas turbines that operate in an open cycle. The two main applications of the Brayton cycle are the jet engine and electric power generation. In the first case, the turbine produces power to drive the compressor and other components, and the exhaust gases at high-speed are accelerated through a nozzle to provide thrust required to propel the aircraft. In the second case, as stationary power plants to generate electricity as independent units or associated with steam power plants when the exhaust gases work as a heat source for the steam. Moreover, the Brayton cycle is also modelled as a closed cycle in nuclear power plants and most naval fleets use gas turbine engines to propel and generate electricity.

The following paragraphs are restricted to studies related to the Brayton cycle applied to space power generation and power generation for hypersonic vehicles. Romano and Ribeiro (2020) propose an optimization of the cold-side temperature of a recuperated closed Brayton cycle (CBC) for space power generation. To this end, a thermodynamic modelling is designed with the recuperator characterized in terms of the effectiveness as a function of temperature, defined as the ratio of the temperature differences at the turbine outlet and the recuperator outlet (energy transferred from the fluid) to the temperature differences at the turbine outlet and the compressor outlet (energy transferred to the fluid).

Considering the heat transfer rate and the heat source temperature as fixed inputs, the aim was to find a cold hot pipe (CHP) temperature that would increase the CBC power output per radiator area. According to the results if the CHP temperature is lower than 400 K, the radiator area would increase tremendously making the system impracticable. Furthermore, the CHP operation temperature reaches a maximum efficiency at $T = 510$ K, which is a balance between a high net power output of the Brayton cycle with a low radiator area.

Cheng *et al.* (2019) intends to optimize the electric power generation for hypersonic vehicles; however, the cold source limits its power, a problem similar to that of Romano and Ribeiro (2020) with the radiator area for space power

generation. The closed Brayton cycle employs supercritical carbon dioxide (S-CO_2) as the working fluid. The compressor supercharges the fluid before entering into the recuperator to absorb the heat from the expanded S-CO_2. Then, combustion takes place in the heater before expanding in the turbine.

The supercritical carbon dioxide is cooled in the precooler until it reaches initial conditions, while the low-temperature fuel absorbs the heat. In the CBC with recompressor, there is the high temperature recuperator (HTR) and the low temperature recuperator (LTR). The compression process is divided into the main compressor and the recompressor, after the working fluid flow through the LTR, one part is cooled in the precooler, as in the simple case, while another part enters the recompressor without cooling.

The Brayton cycle modelling in Cheng *et al.* (2019) is similar to that adopted in the present work, using isentropic efficiencies of the compressor and turbine to determine states 2 and 4. In addition, the recuperator effectiveness is defined as the ratio of the actual heat transfer rate to the theoretical maximum value. The enthalpy of the expanded fluid leaving the recuperator is evaluated considering the exit pressure and the temperature of the compressed fluid.

The authors Cheng *et al.* (2019) conclude that the compressor inlet temperature with a finite cold source is far higher than S-CO_2 compressors in general, and the maximum value for temperature is 389 K in the simple recuperated Brayton cycle. When compared both the recuperated closed Brayton cycle and the Brayton cycle with recompressor, it is more feasible to develop the simple recuperated Brayton cycle taking into account the inferiority in structural complexity on hypersonic vehicles and the electric power generation.

The Brayton cycle is usually modelled by operating with air for all states. The objective of the present work is to evaluate the Brayton cycle with a recuperator, modelling the combustion process using chemical equilibrium to determine the composition of the combustion products. From this evaluation, the behavior of polluting gases and the thermal efficiency of the cycle are analysed with respect to the variation in the effectiveness of the recuperator. Thus, this analysis allows to balance the cycle efficiency and the emission of pollutant gases.

2. METHODOLOGY

The thermodynamic and combustion aspects regarding the Brayton cycle with recuperator was numerically modelled. Firstly, we present a brief description of the Brayton cycle. Then, in a second moment, it follows the mathematical equations, combustion modelling, numerical algorithm and real input data.

2.1 Description of the Brayton cycle with recuperator

The compressor admits fresh air at state 1 - at the standard pressure (lower isobaric line in Fig. 1b) and temperature. The admitted air undergoes compression work, raising the fluid pressure to the operating pressure (the higher isobaric line in Fig. 1b) of the combustion chamber, and increasing the temperature in the process.

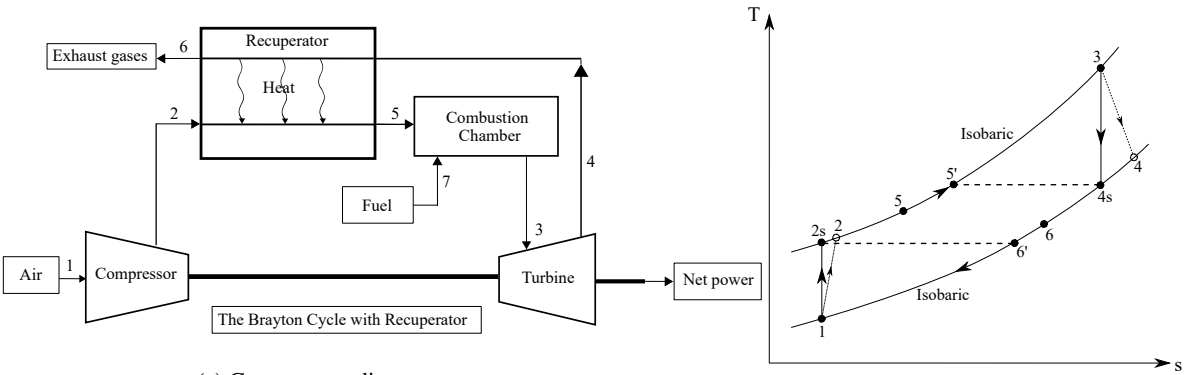

(a) Components diagram.

(b) Temperature-entropy diagram.

Figure 1. The Brayton cycle with recuperator (Adapted from Çengel and Boles (2007)).

Compressed air at high pressure (state 2) enters a combustion chamber; fuel (state 7) is injected into the air (oxidizer) and the reaction takes place at constant pressure. The exothermic reaction releases energy in the form of heat into the cycle, and at the end of the combustion process (state 3) occurs the highest temperature in the cycle (T_3), limited by the temperature that the turbine blades can withstand.

Then, the combustion gases at high temperature and pressure expand through several stages in the gas turbine, producing work. A fraction of the work is transmitted by the shaft to operate the compressor and the remaining work is the net work output of the Brayton cycle (net power), as shown in Fig. 1a.

The exhaust gases leave the turbine at atmospheric pressure being discharged to the atmosphere, configuring an open cycle. However, the outlet temperature of the gases in a simple Brayton cycle is well above ambient temperature, as a

result, the energy in the form of heat from the combustion products would be irretrievably lost if the gases were discharged to the atmosphere.

The recuperated Brayton cycle recuperates part of the heat that would be lost in the atmosphere in order to preheat the compressed air before it enters the combustion chamber, using a recuperator that is a countercurrent heat exchanger.

The hot gases from the turbine exhaust line exchange heat with the cool air leaving the compressor in a heat exchanger, normally in parallel pipes, flowing in opposite directions. The exhaust gases are cooled from state 4 to state 6, while the air leaving the compressor is heated from state 2 to state 5 before state 3, as presented in Fig. 1a. To allow heat transfer, the temperature at state 2 must be less than the temperature at state 4 ($T_2 < T_4$).

Thus, with a recuperator, less chemical energy from the fuel is used to heat the incoming oxidizer in the combustion chamber. This implies higher adiabatic flame temperatures and higher T_3 values. The net work produced is not changed by the addition of a recuperator; however, it reduces the added heat, and therefore the thermal efficiency of the cycle increases. Also, another approach would be to reduce the amount of fuel while maintaining the same thermal efficiency of the cycle without a recuperator, which is usually the case in practice.

At the end, the exhaust gases leave the recuperator entering the atmosphere (state 6) at a lower temperature than T_4 and at atmospheric pressure. In summary, the isentropic Brayton cycle behavior considering an ideal recuperator follows the states sequence 1–2s–5âĂŹ–3–4s–6' whereas the Brayton cycle behavior including compressor and gas turbine irreversibilities and considering an actual efficiency in the recuperator follows the states sequence 1–2–5–3–4–6.

2.2 Modelling of the Brayton cycle with recuperator

Thermodynamic modelling consists of a compressor, a combustion chamber, a gas turbine, and a recuperator. Each of these components is analyzed as a control volume, at steady state condition. The compression and expansion processes are adiabatic, the pressure drop during the heat addition process and head losses are not considered.

Due to irreversibilities, the real compression work required to take pressure to the upper isobaric pressure line increases and the real work produced by the turbine decreases. Considering the irreversibility effects, it is used isentropic efficiencies for the compressor and the gas turbine. Standard air is defined as 21 $\%$ oxygen and 79 $\%$ nitrogen, which means 3.76 moles of N_2 for each mole of O_2.

The methodology used to solve numerically the properties of combustion products is based on a method applied by Olikara and Borman (1975), using equilibrium constants for gas-phase combustion products of hydrocarbon fuels. The modelling of combustion reactions is done as described by Ferguson and Kirkpatrick (2016).

According to Ferguson and Kirkpatrick (2016) the product species of importance resulting from dissociation are O, H, OH and NO. Therefore, it is necessary to consider only 10 significant product species, they are presented by:

$$\begin{aligned} C_aH_bO_cN_d + \frac{a_s}{\phi}(O_2 + 3.76N_2) \rightarrow n_1CO_2 + n_2H_2O + n_3N_2 + n_4O_2 + n_5CO + \\ n_6H_2 + n_7H + n_8O + n_9OH + n_{10}NO \end{aligned} \tag{1}$$

Where a_s is the stoichiometric molar air-fuel ratio, ϕ is the fuel-air equivalence ratio defined as the actual fuel-air ratio (FA) divided by the stoichiometric fuel-air ratio (FA_s):

$$\phi = \frac{FA}{FA_s} \tag{2}$$

When $\phi = 1$ the mixture is stoichiometric, that is, a balanced mixture of fuel and oxidizer (air) such that no excess of either remains after combustion. If $\phi < 1$, the mixture is lean (lack of fuel), and if $\phi > 1$, the mixture is rich (excess of fuel). From the principle of mass conservation, we know that atoms are conserved; therefore, balancing the atoms generates the following equations:

$$\begin{aligned} C: &\quad a = (y_1 + y_5)N \\ H: &\quad b = (2y_2 + 2y_6 + y_7 + y_9)N \\ O: &\quad c + 2\frac{a_s}{\phi} = (2y_1 + y_2 + 2y_4 + y_5 + y_8 + y_9 + y_{10})N \\ N: &\quad d + 7.52\frac{a_s}{\phi} = (2y_3 + y_{10})N \end{aligned} \tag{3}$$

The gas-phase equilibrium reactions are the dissociation of hydrogen, oxygen, water, carbon dioxide, and the formation of OH and NO. These reactions provide six additional equations to the four equations from the atomic species balance, previously presented in Eq. (3).

$$
\begin{aligned}
&\tfrac{1}{2}H_2 \rightleftharpoons H && K_1 = \frac{y_7 P^{1/2}}{y_6^{1/2}} \\
&\tfrac{1}{2}O_2 \rightleftharpoons O && K_2 = \frac{y_8 P^{1/2}}{y_4^{1/2}} \\
&\tfrac{1}{2}H_2 + \tfrac{1}{2}O_2 \rightleftharpoons OH && K_3 = \frac{y_9}{y_4^{1/2} y_6^{1/2}} \\
&\tfrac{1}{2}O_2 + \tfrac{1}{2}N_2 \rightleftharpoons NO && K_4 = \frac{y_{10}}{y_4^{1/2} y_3^{1/2}} \\
&H_2 + \tfrac{1}{2}O_2 \rightleftharpoons H_2O && K_5 = \frac{y_2}{y_4^{1/2} y_6 P^{1/2}} \\
&CO + \tfrac{1}{2}O_2 \rightleftharpoons CO_2 && K_6 = \frac{y_1}{y_4^{1/2} y_5 P^{1/2}}
\end{aligned}
\tag{4}
$$

The unit of pressure in Eq. (4) is the atmosphere (atm). The equilibrium constant curve-fit coefficients are obtained by regression based on the data in the *JANAF Tables* for the temperature range 600 < T < 4000 K, and presented by Ferguson and Kirkpatrick (2016). The expressions for $K_i(T)$ are:

$$\log_{10} K_i(T) = A_i \ln\left(\frac{T}{1000}\right) + \frac{B_i}{T} + C_i + D_i T + E_i T^2 \tag{5}$$

Equations (3) and (4) are a set of ten nonlinear equations for the ten unknowns (y_i). The system of nonlinear equations is implemented through Scilab© routines using the *fsolve* function, the initial required value is considered to be the stoichiometric solution which increases the convergence of the algorithm.

The sum of moles of all *n* components is the total number of moles of the mixture (*N*):

$$N = \sum_{i=1}^{n} n_i \tag{6}$$

Dividing the number of moles of each component by the total number of moles results in the mole fraction, y_i, of each component, results:

$$y_i = \frac{n_i}{N} \tag{7}$$

The molar mass of the mixture, *M* (kg/kmol), is the sum of the products of the molar fraction and the molar mass of each component:

$$M = \sum_{i=1}^{n} y_i M_i \tag{8}$$

The specific gas constant of the mixture R (kJ/kg K) is given by the molar universal gas constant (R_u = 8.314 kJ/kmol K) divided by the molar mass of the mixture, which results:

$$R = \frac{R_u}{M} \tag{9}$$

If the mixture composition, that is, the mole fractions are known, the thermodynamic properties *(c_p, h, u, s and v)* can be determined. Firstly, the constant pressure specific heat of the mixture depends on the change in enthalpy and it is sensitive to the change in mixture composition as a function of temperature. The equation to describe c_p (kJ/kg K) is:

$$c_p = \frac{1}{M}\left[\sum_{i=1}^{n} y_i \overline{c}_{p_i} + \sum_{i=1}^{n} \overline{h}_i \frac{\partial y_i}{\partial T} - \frac{\overline{h}}{M}\sum_{i=1}^{n} M_i \frac{\partial y_i}{\partial T}\right] \tag{10}$$

In order to calculate the first term in Eq. (10), it is necessary to determine the specific heat for each species.

Specific heats of various species have been curve-fitted to polynomials. In this paper, the curve-fit coefficients *(a_i)* are based on data, as presented by Ferguson and Kirkpatrick (2016), for temperature ranges 300 $\leq$ T < 1000 K and 1000 $\leq$ T $\leq$ 3000 K.

For any given species, the molar specific heat is approximated by:

$$\overline{c}_{p_i} = R_u(a_1 + a_2T + a_3T^2 + a_4T^3 + a_5T^4) \tag{11}$$

The thermodynamic relations for an ideal gas are $dh = c_p dT$ and $ds = (c_p/T)dT$, thus, the mathematical expressions for specific enthalpy and specific entropy are found by integration. The enthalpy of each component *i*, on a molar basis, is given by:

$$\overline{h}_i = R_u T\left(a_1 + \frac{a_2}{2}T + \frac{a_3}{3}T^2 + \frac{a_4}{4}T^3 + \frac{a_5}{5}T^4 + \frac{a_6}{T}\right) \tag{12}$$

The mixture's specific entalphy *h* (kJ/kg):

$$h = \frac{1}{M}\sum_{i=1}^{n} y_i\overline{h}_i \tag{13}$$

The molar specific entropy of each component *i*, $\overline{s}_i$ (kJ/kmol K):

$$\overline{s}_i(T,P) = \overline{s}_i^{\circ}(T) - Ru\ ln\left(P_i/P_{\circ}\right) \tag{14}$$

Where P_i is the partial pressure and $P_{\circ}$ is the atmospheric pressure ($P_{\circ}$ = 101.325 kPa). The first term in Eq. (14) is the formation entropy, $\overline{s}_i^{\circ}(T)$, given by:

$$\overline{s}_i^{\circ} = R_u\left(a_1 \ln T + a_2T + \frac{a_3}{2}T^2 + \frac{a_4}{3}T^3 + \frac{a_5}{4}T^4 + a_7\right) \tag{15}$$

The partial pressure is the pressure that a species would exert if it occupied the entire volume of the mixture at a given temperature. Partial pressure for each species:

$$P_i = y_i\ P \tag{16}$$

Once the molar specific entropy of *i* components is evaluated at its pressure and as a function of temperature in Eq. (14), the mixture's entropy is determined.

The specific entropy *s* (kJ/kg K) of the mixture is the sum of the product of the molar entropy of each component and its respective mole fraction divided by the molar mass of the mixture:

$$s = \frac{1}{M}\sum_{i=1}^{n} y_i\overline{s}_i \tag{17}$$

The relationship between pressure, temperature, and volume for an ideal gas is $Pv = R\,T$. And therefore, the specific volume of the mixture, *v* (m^3/kg), is given by:

$$v = \frac{R_u\ T}{P\ M} \tag{18}$$

Finally, the specific internal energy of the mixture *u* (kJ/kg) is determined:

$$u = h - Pv \tag{19}$$

Once the composition and thermodynamic properties of the mixture have been determined. Thermodynamic states are evaluated. At the beginning of the cycle, air enters the compressor at ambient temperature (T_1 = 300 K) and atmospheric pressure ($P_1 = P_{\circ}$). Given these values and the air composition defined, the thermodynamic properties at state 1 are determined.

At state 2, the exit pressure (P_2) is calculated:

$$P_2 = r_{cp}P_1 \tag{20}$$

Where r_{cp} is the compressor pressure ratio, given in the Tab. 1.

The compression process 1–2 is isentropic and, therefore, $s_1 = s_{2s}$. The entropy (s_{2s}) depends on the theoretical temperature (T_{2s}) and pressure for state 2. The temperature T_{2s} is the only unknown variable, but as the relationship is not direct an algorithm was developed based on the Newton-Raphson iterative method in order to find the value of T_{2s} for which s_{2s} is equal to s_1.

The method begins with an arbitrary initial temperature and the entropy $s_{2s}(T_{2s_i}, P_2)$ is calculated, and then compared with $s_1(T_1, P_1)$, the algorithm evaluates whether the Newton-Raphson step assures a downward direction; otherwise, half

a step is taken. The iterative method repeats itself until the difference between entropies respects a predetermined tolerance ($s_1 - s_{2s} < tol$). When tolerance is reached, there is $s_{2s} = s_1$, and from T_{2s}, the theoretical enthalpy for the second state (h_{2s}) is found.

Based on the compressor isentropic efficiency (η_c), the real enthalpy (h_2) is determined:

$$h_2 = \frac{h_{2s} - h_1}{\eta_c} + h_1 \tag{21}$$

Following the same approach for calculating T_{2s}, the compressor exit temperature (T_2) is obtained through the iterative method from the known variables h_2 and P_2. Thus, all the thermodynamic properties at state 2 are determined. In the first iteration, the program is run for a simple Brayton cycle considering the compressor output values as the input values in the combustion chamber and from the second iteration on, the recuperator modelling is used since it requires the enthalpy at state 4.

The recuperator effectiveness (η_{rec}) is a parameter that measures the distance between an ideal recuperator and a real recuperator. It is defined as the ratio between the actual increase in enthalpy of the air flowing through the compressor side of the recuperator ($q_{rec,real}$) to the maximum theoretical enthalpy change in an ideal recuperator ($q_{rec,max} = h_{5'} - h_2 = h_4 - h_2$).

The enthalpy unit at states 2 and 5 is $\mathrm{kJ/kg_{air}}$. For the sake of consistency, in Eq. (22), the enthalpy ($h_{4,air}$) simulate the air enthalpy at state 4, which is the upper energetic limit:

$$\eta_{rec} = \frac{q_{rec,real}}{q_{rec,max}} = \frac{h_5 - h_2}{h_{4,air} - h_2} \tag{22}$$

This value provides the maximum thermal potential, that is, the maximum available heat that can be transferred to the air flowing through the recuperator. The maximum theoretical value for the temperature of air (T_5) is the exit temperature in the turbine (T_4), when maximum heat transfer occurs, $h_5 \rightarrow h_{4,air}$ and $\eta_{rec} = 100\ \%$. In this case, the combustion products would leave the recuperator at $T_{6'} = T_2$.

According to Moran *et al.* (2013), typical values for the effectiveness of the recuperator are between 60 % to 80 %, and thus the temperature of the air (T_5) leaving the recuperator is below T_4. After h_5 is determined in Eq. (22) and as the heat transfer process takes place at constant pressure, T_5 is found by the iterative method and all other thermodynamic properties at state 5 are calculated.

In the cycle, the most significant irreversibilities occur during the combustion process and they are represented by the efficiency of the combustion chamber (η_{cb}). The chemical energy (kJ/s) of the injected fuel, in this case, methane (CH_4) whose properties can be seen at Gama (2017), is given by:

$$\dot{Q}_f = \dot{m}_f LHV \tag{23}$$

Where *LHV* refers to the Lower Heating Value of a fuel ($LHV_{\mathrm{CH_4}} = 50\,019.93$ kJ/kg), and $\dot{m}_f$ ($\mathrm{kg\ _{fuel}/s}$) is the fuel mass flow rate. The energy balance in the combustion chamber is presented by Eq. (24) and demonstrated by Ziółkowski *et al.* (2013), where $\dot{m}_a$ ($\mathrm{kg\ _{air}/s}$) is the air mass flow rate, the entalphy (h_{comb}) is based on the air properties at T_{amb} = 300 K, and $\dot{m}_{ex}$ ($\mathrm{kg\ _{mixt}/s}$) is the exhaust gas mass flow rate and defined as $\dot{m}_{ex} = \dot{m}_a + \dot{m}_f$.

$$h_{3i} = \frac{\eta_{cb}\left(\dot{Q}_f + \dot{m}_a h_5 + \dot{m}_f h_{comb}\right)}{\dot{m}_{ex}} \tag{24}$$

The process 2–5–3 is isobaric ($P_2 = P_5 = P_3$) and with the reference enthalpy (h_{3i}) calculated in Eq. (24), the same reasoning from state 2 is employed to find the temperature of the gases leaving the combustion chamber (T_3).

The same iterative method is used starting with an arbitrary initial temperature above (T_5) and calculating the enthalpy of the mixture, however, considering the combustion products as modelled above. This value is then compared to h_{3i} and the process is repeated until tolerance is reached, T_3 is known and the thermodynamic properties at state 3 are determined.

The expansion process in the turbine (3–4) is considered to be ideal and isentropic, thus $s_3 = s_{4s}$. The theoretical temperature of the combustion gases at the turbine outlet is found by a temperature initial (arbitrary) guess and then comparing $s_{4s}(T_{4s}, P_4)$ to s_3 until the correct temperature value is reached so that tolerance is respected.

The pressure (P_4) of the exhaust gases leaving the turbine is a system input data. In the simple Brayton cycle, atmospheric pressure is usually considered. In this case, however, the gas will flow through the recuperator before exiting the atmosphere, so it is necessary that the pressure at state 4 is above the atmospheric pressure ($P_6 = P_1$).

It is noted through bibliographic research that, generally, for theoretical purposes, the pressure in the recuperator is considered equal to the atmospheric pressure. In the present work, it is used a pressure drop factor developed analytically by Marija *et al.* (2017), which establishes Eq. (25), where the term in the denominator is a non-dimensional pressure drop in the hot side of the recuperator. Since P_6 and n_{rec} are input data, P_4 is calculated:

$$P_4 = \frac{P_6}{1 - 0.005859\left(\frac{\eta_{rec}}{1-\eta_{rec}}\right)} \tag{25}$$

In a similar way to state 2, with T_{4s} it is possible to determine the theoretical enthalpy h_{4s}. Based on the turbine isentropic efficiency (η_t), the real enthalpy (h_4) is determined:

$$h_4 = \eta_t(h_{4s} - h_3) + h_3 \tag{26}$$

Using the same iterative rationale, the corresponding temperature (T_4) that takes enthalpy to h_4 is found, and all thermodynamic properties at state 4 are known. Since part of the energy of the exhaust gases is transferred to the air, a comparison is made $T_4^j - T_4^{(j-1)} < tol$, and if the difference between temperatures at state 4 is inferior to pre-established tolerance, the algorithm stops; otherwise, additional iterations are needed, as there is still potential for the recuperator to recuperate the heat from the hot side to increase the value of h_5.

To find out how much energy the combustion gases supplied to the compressed air, the heat gained by the air between states 2 and 5 in Eq. (27) is determined. And as state 4 is known, the enthalpy of the exhaust gases (h_6) that leaves the recuperator is calculated in Eq. (28).

$$Q = h_5 - h_2 \tag{27}$$

$$h_6 = h_4 - Q \tag{28}$$

Enthalpy and pressure are known at state 6 and, therefore, it is employed the equilibrium module and the Newton-Raphson method to find the temperature value that takes enthalpy to h_6, once solved, T_6 is found and all the thermodynamic properties for state 6.

All states are determined and the thermal efficiency of the cycle can be calculated. But first, the work done by the compressor (W_c) and the work produced by the gas turbine (W_t) are defined as:

$$W_c = \frac{h_{2s} - h_1}{\eta_c} \tag{29}$$

$$W_t = \eta_t(h_3 - h_{4s}) \tag{30}$$

The net work (W_{net}) output of the cycle is given by Eq. (31). And the fraction of work produced by the gas turbine and consumed by the compressor is the back work ratio (bwr) for the Brayton cycle, presented by Eq. (32).

$$W_{net} = W_t - W_c \tag{31}$$

$$bwr = \frac{W_c}{W_t} \tag{32}$$

At last, the thermal efficiency of the cycle (η_{th}) is given by:

$$\eta_{th} = \frac{W_t\dot{m}_{ex} - W_c\dot{m}_a}{\dot{Q}_f} \tag{33}$$

Where $\dot{Q}_f$ is the amount of energy generated by the fuel, defined in Eq. (23).

2.3 Input data and algorithm overview

The input data required to determine all cycle states is presented in the Tab. 1, and based on real operational conditions of a thermoelectric plant, described by Branco (2005).

Table 1. Input data for the Brayton cycle modelling (Branco, 2005).

Input	Value	Input	Value
Compressor isentropic efficiency (η_c)	87 %	Compressor pressure ratio (r_{cp})	14.5
Combustion chamber efficiency (η_{cb})	90 %	Air mass flow rate ($\dot{m}_a$)	197.5 kg/s
Turbine isentropic efficiency (η_t)	92 %	Fuel mass flow rate ($\dot{m}_f$)	4.71 kg/s
Combustion products mass flow rate ($\dot{m}_{ex}$)	202.21 kg/s	Fuel-air equivalence ratio (ϕ)	0.8

The algorithm exemplifying the reasoning used to develop the computational modelling is presented in Fig. 2.

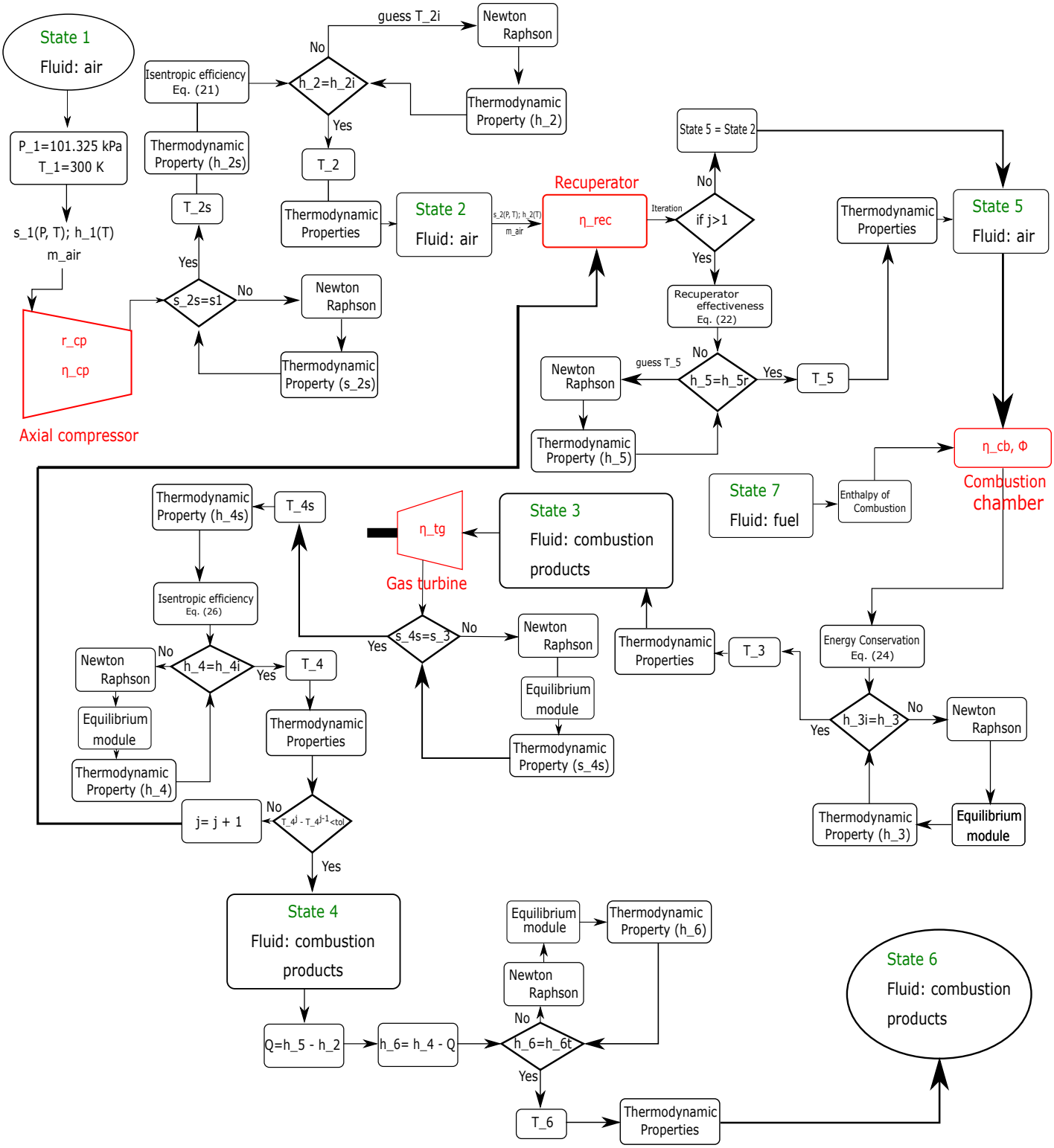

Figure 2. The Brayton cycle with recuperator and combustion algorithm.

3. RESULTS AND DISCUSSION

The modelling of the Brayton cycle considering combustion and recuperator, with the input data from Tab. 1 is simulated for different effectiveness of the recuperator. As previously stated, the real effectiveness is in the range between 60 and 80 %, thus the effectiveness considered are 0.4, 0.6 and 0.8. In addition, it is also simulated for both cases without a recuperator ($\eta_{rec} = 0$) and with an ideal recuperator ($\eta_{rec} = 1$).

Ferro *et al.* (2019) also simulates the simple Brayton cycle disregarding combustion and only considering pure air, process 1 and 2 remain the same since the combustion chamber is represented by state 3 and the cycle thermal efficiency is 30.62 %, a decrease of 28 % compared to the simple Brayton cycle with combustion modelling. In the case without recuperator and with combustion, the present results matches with those obtained by Ferro *et al.* (2019), which uses the same modelling for the Brayton cycle, considering only combustion. The results for the thermal efficiency of the cycle varying according to the various effectiveness of the recuperator are shown in Fig. 3.

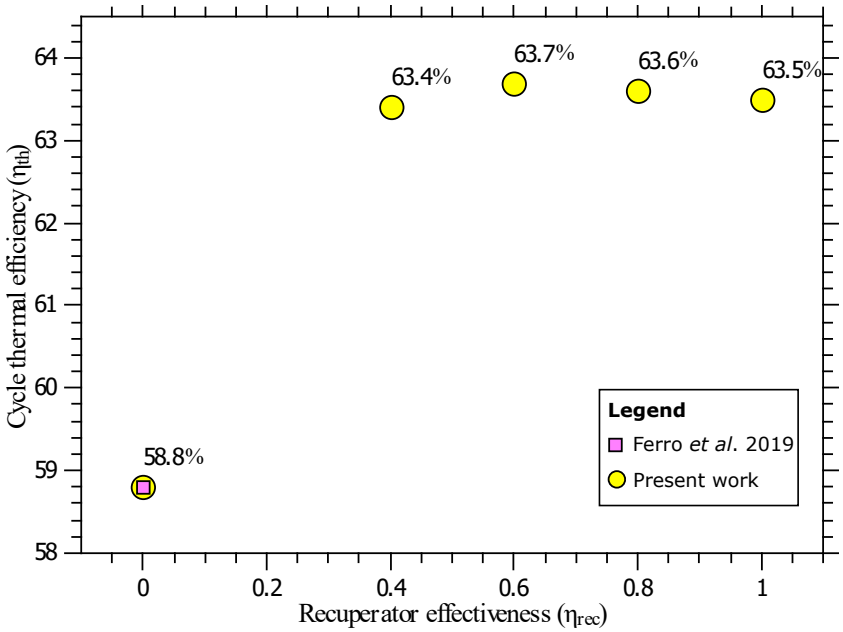

Figure 3. Cycle efficiency sensitivity to the recuperator effectiveness.

When the recuperator is added, the thermal efficiency of the cycle rises since part of the energy that would be wasted is used to heat the compressed air. The square marker in Fig. 3 represents the result obtained by Ferro *et al.* (2019) for the cycle without the recuperator, an increase of almost 5 % is noted for any effectiveness value of the recuperator above 40 %. It is important to note that the thermal efficiency of the recuperated cycle remains virtually constant regardless of the effectiveness of the recuperator for the evaluated ranges. Equation (33) sheds some light on the constant behavior of the cycle thermal efficiency.

The addition of the recuperator does not modify the compression work at state 2, nor the mass flow rates of air and fuel. Another parameter that remains constant is the chemical energy of the fuel given by Eq. (23). Therefore, the only variable in Eq. (33) is the work produced by the gas turbine and given by Eq. (30). The turbine isentropic efficiency is constant and, thus, it is necessary to assess the enthalpy variations at states 3 and 4.

Figure 4 illustrates the enthalpy variations for each recuperator effectiveness, as well as temperature variations. The presence of the recuperator influences state 3. This effect is observed when enthalpy at state 3 (h_{3i}) is calculated, since the term ($\dot{m}_a h_5$) in Eq. (24) contains information of the state 5. The enthalpy h_{3i} has a gain due to h_5, and at the end of the combustion occurs the highest temperature value in the cycle, before the combustion gases expand in the turbine and leave at T_4, which is above T_5, as illustrated in Fig. 4a.

As the effectiveness of the recuperator increases, the rate of heat transferred to the air in the recuperator increases. Therefore, the higher the effectiveness of the recuperator, the higher the temperature T_5, and consequently T_3 e T_{4s}, will be higher than before. According to the present numerical model, the temperatures rise is nearly constant.

Enthalpies h_3 and h_{4s} are dependent on both temperature and pressure when determining chemical equilibrium, while h_5 depends only on temperature because it is only air at state 5. In Fig. 4a there is an overlap for temperatures T_5 and T_{4s} when $\eta_{rec} = 1$, the difference is small and the numerical values can be interpreted as the same, since the difference obtained may have risen from numerical error.

Even though the temperatures and the corresponding enthalpies rise by the presence of the recuperator, the thermal efficiency of the cycle remains constant due to the fact that the work on the turbine (the only variable in the equation) is

the difference in enthalpies ($h_3 - h_{4s}$). The pressures remain constant for all ranges of effectiveness and thus the enthalpy varies only due to the temperatures, but even with an increase in enthalpies, the difference between them remains constant as can be observed in Fig. 4b.

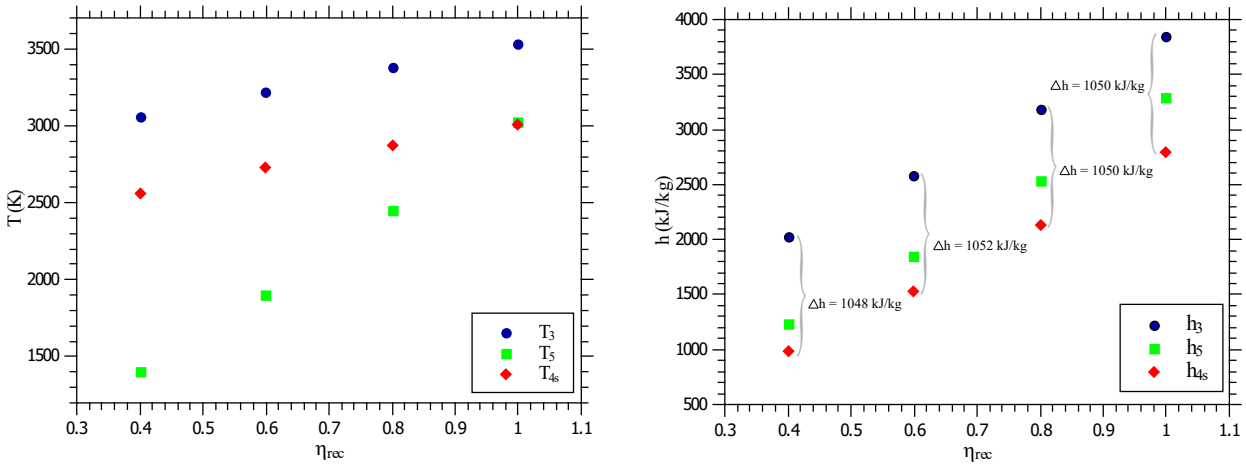

(a) Temperature sensitivity to the recuperator effectiveness.

(b) Enthalpy sensitivity to the recuperator effectiveness.

Figure 4. Sensitivity of temperature and enthalpy to the recuperator effectiveness.

Due to the concern regarding environmental issues, another point that shall be mentioned is the pollutant emissions. Figure 5 illustrates the concentration of [CO] and [NO] gases when they are discharged into the atmosphere at state 6. The [CO] concentration remains below 0.2 %, regardless of the recuperator effectiveness, due to the combustion products temperature (T_6) behavior. The temperature scale is represented on the right y-axis. As the recuperator effectiveness increases, the heat transferred from the combustion products is higher, thus, decreasing the exhaust temperatures. The [NO] concentration is almost 0.5 % for the lowest recuperator effectiveness and it is reduced by 30 % for the ideal case. Lastly, for the case without recuperator, the combustion products do not transfer heat to the air and, therefore, the outlet temperature of the turbine (T_4) is higher than T_6, the [CO] and [NO] emissions follow the same behavior, higher than all evaluated cases with recuperator.

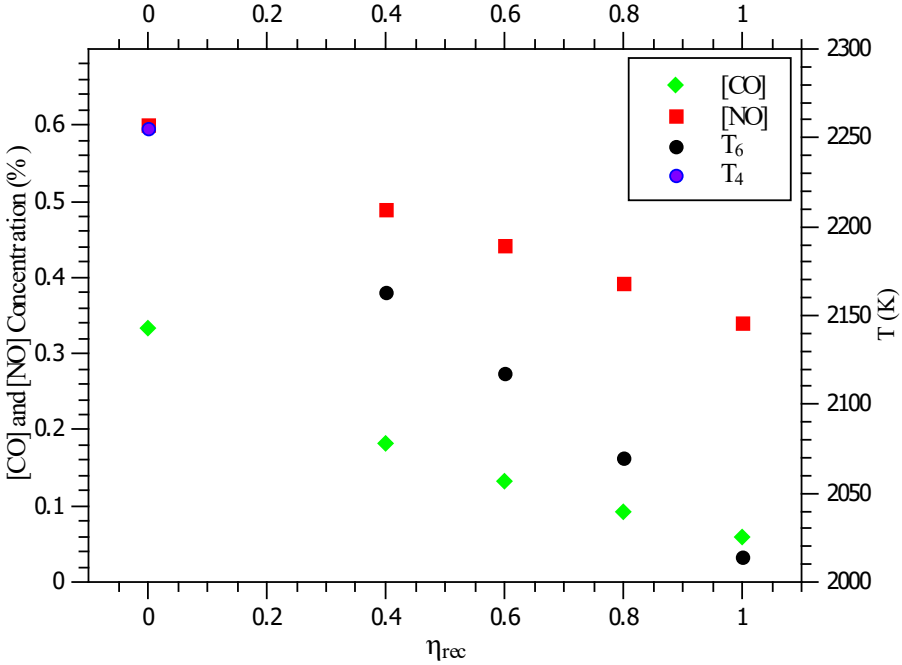

Figure 5. Sensitivity of emission and exhaust temperature to the recuperator effectiveness.

As shown in Fig. 5, even with the addition of a recuperator, the exhaust gas temperature (T_6) is above 2000 K for all evaluated cases.

It is important to evaluate the [CO] and [NO] emissions for the maximum emission limits for air pollutants determined by the National Regulatory Agency (CONAMA) in Brazil. To draw the comparison, the effectiveness of the recuperator is kept fixed at $\eta_{rec} = 0.8$ and the concentration of the pollutants with respect to the T_6 temperatures are illustrated in Fig. 6.

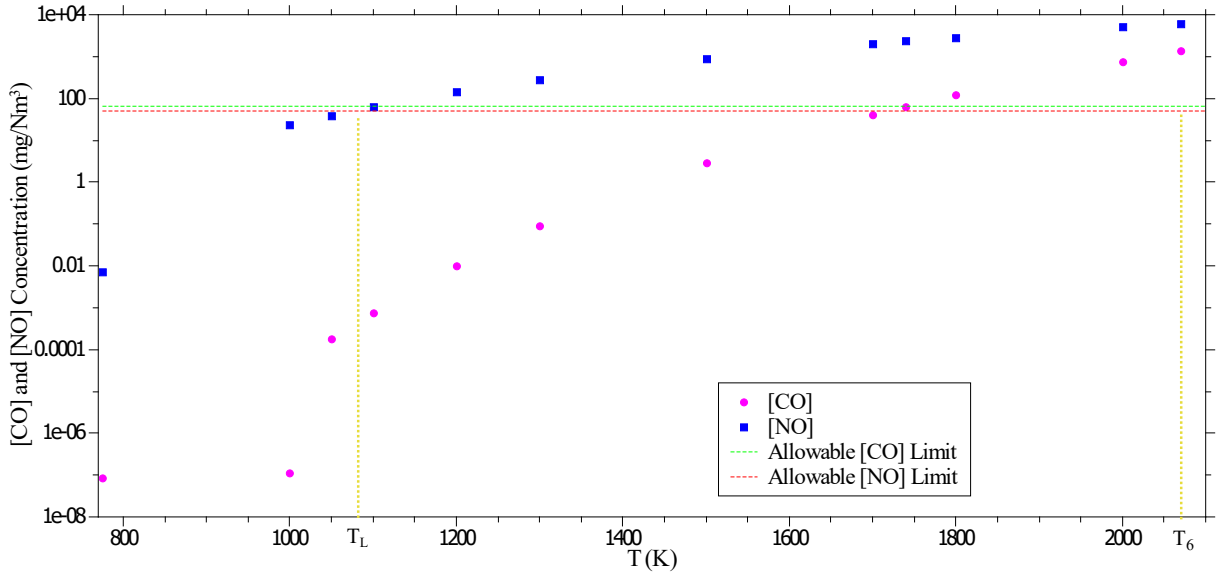

Figure 6. Emission limits according to the national regulatory agency CONAMA.

Allowable emission limits from gas turbines operating on natural gas for electricity generation with electrical power above 100 MW is presented by the dashed lines in Fig. 6. According to CONAMA (2006), the concentration limit for [CO] is 65 $\mathrm{mg/Nm^3}$ and the concentration limit for [NO] is 50 $\mathrm{mg/Nm^3}$.

The [CO] concentration for temperatures below 1300 K are less than 99 $\%$ of the CONAMA's upper limit, there is a considerable increase for temperatures above 1500 K reaching the maximum upper limit (65 $\mathrm{mg/Nm^3}$) at a temperature of approximately 1750 K. The [NO] emissions are higher and reach the concentration limit at a temperature of approximately 1080 K (T_L). For the combustion gases temperature above 2000 K at state 6, the second vertical dashed line, it is observed that the concentrations of [CO] and [NO] are well above the allowed limits. For this reason, as well, it is feasible to use a secondary recuperator to lower the outlet temperature of the combustion products and, consequently, reduce emissions to a secure level.

4. CONCLUSIONS

The present model suggests that there is almost a 5-percent increase to the Brayton cycle efficiency with the addition of a recuperator, regardless of its effectiveness. The recuperator effectiveness demonstrated, nevertheless, great impact on the emissions control strategy. According to the present model, a single recuperator is still not enough to reduce the exhaust gases temperature and pollutant emission levels. Further treatment for the exhaust gases are necessary.

5. ACKNOWLEDGEMENTS

The authors thank UFGD for making this work possible.

6. REFERENCES

Branco, F.P., 2005. *Análise termoeconômica de uma usina termelétrica a gás natural operando em ciclo aberto e em ciclo combinado*. Ph.D. thesis, Universidade Estadual Paulista, Ilha Solteira, Brasil. doi:10.13140/RG.2.1.2590.5042.

Çengel, Y.A. and Boles, M.A., 2007. *Termodinâmica*. McGraw Hill, 5th edition.

Cheng, K., Qin, J., Sun, H., Li, H., He, S., Zhang, S. and Bao, W., 2019. "Power optimization and comparison between simple recuperated and recompressing supercritical carbon dioxide Closed-Brayton-Cycle with finite cold source on hypersonic vehicles". *Energy*, Vol. 181, pp. 1189–1201. ISSN 0360-5442. doi:10.1016/j.energy.2019.06.010.

CONAMA, 2006. "ResoluÃğÃčo no 382". URL `http://www2.mma.gov.br/port/conama/res/res06/res38206.pdf`. [Online; accessed 02. Aug. 2020].

Ferguson, C.R. and Kirkpatrick, A.T., 2016. *Internal combustion engines: applied thermosciences*. John Wiley & Sons, 3rd edition.

Ferro, B.A.P.C., Ramos, R.A.V. and Bornschlegell, A.S., 2019. "Thermoelectric powerplant performance and emission control simulation". *CILAMCE 2019, Natal-RN*.

Gama, G., 2017. "Propriedade dos gases: Metano". URL `http://www.gamagases.com.br/propriedades-dos-gases-metano.html`. [Online; accessed 15. Jul. 2020].

Marija, Z., Virag, Z. and Galovic, A., 2017. "Another view on the optimization of the brayton cycle with recuperator". *Tehnicki Vjesnik*, Vol. 24, pp. 419–425. doi:10.17559/TV-20160520115040.

Moran, M.J., Shapiro, H.N., Boettner, D.D. and Bailey, M.B., 2013. *Princípios de termodinâmica para engenharia*. LTC Editora, 7th edition.

Olikara, C. and Borman, G.L., 1975. "A Computer Program for Calculating Properties of Equilibrium Combustion Products with Some Applications to I.C. Engines". In *SAE Technical Paper*. SAE International. ISSN 0148-7191. doi:10.4271/750468. [Online; accessed 23. Jul. 2020].

Romano, L.F.R. and Ribeiro, G.B., 2020. "Cold-side temperature optimization of a recuperated closed Brayton cycle for space power generation". *Thermal Science and Engineering Progress*, Vol. 17. ISSN 2451-9049. doi:10.1016/j.tsep.2020.100498.

Ziółkowski, P., Zakrzewski, W., Dolna, O. and Badur, J., 2013. "Thermodynamic analysis of the double brayton cycle with the use of oxy combustion and capture of CO2". *Archives of Thermodynamics*, Vol. 34, pp. 23–38. doi:10.2478/aoter-2013-0008.

7. RESPONSIBILITY NOTICE

The authors are solely responsible for the printed material included in this paper.